Working fluid selection and performance comparison of subcritical and supercritical organic Rankine cycle (ORC) for low-temperature waste heat recovery

Stéphanie Jumel
EDF – Recherche et Développement
Département Eco-efficacité des Procédés Industriels
Site des Renardières
77818 Moret sur loing Cedex
France
stephanie.jumel@edf.fr

Van Long Le (corresponding author)
Theoretical and Applied Energy and Mechanics Laboratory
CNRS, LEMTA, UMR 7563
F-54500 Vandoeuvre-lès-Nancy
France
van-long.le@univ-lorraine.fr

Michel Feidt
Theoretical and Applied Energy and Mechanics Laboratory
CNRS, LEMTA, UMR 7563
F-54500 Vandoeuvre-lès-Nancy
France
michel.feidt@univ-lorraine.fr

Abdelhamid Kheiri
Theoretical and Applied Energy and Mechanics Laboratory
CNRS, LEMTA, UMR 7563
F-54500 Vandoeuvre-lès-Nancy
France
abdelhamid.kheiri@univ-lorraine.fr

Keywords

waste heat, industrial processes, heat recovery

Abstract

In the industrial and daily processes, a big amount of energy is lost as waste heat. This heat source reduces not only the energy efficiency of industrial process but it also contributes to greenhouse gases emissions and thermal pollution. In this context, the CERES project (Energy pathways for waste heat recovery in industrial systems), financed by the French National Research Agency, aims at developing a decision-making tool to optimize waste heat recovery in industrial process. Through this platform, the comparison of various technologies (heat pumps, thermoelectricity, ORC …) based on technico-economic basis will be possible.

In the article, it is proposed to describe one of these technologies, the Organic Rankine Cycles (subcritical and supercritical cycle), which can be used to valorize low-temperature waste heat.

The Organic Rankine Cycle performances were analyzed and compared via their thermal efficiencies and exergy analysis. Both of these cycles used a heat source simulated by hot air with an inlet temperature of 170 °C and a heat sink that is water at ambient temperature to cool down and condense the working fluid. The performance calculations and the cycle simulation were carried out by Engineering Equation Solver (EES).

Introduction

Nowadays, just as world population is growing, so is world energy consumption. According to the New Policies Scenario in world energy outlook 2011 (IEA 2011), world primary energy demand is projected to increase from 12,150 Mtoe in 2009 to 16,950 Mtoe in 2035, an increase of 40 %, or 1.3 % growth per year . Consequently, solutions to face fossil fuels run out have to be found. Nuclear energy can contribute to meeting the growing demand for energy, but safety and nuclear waste treatment constrains are also limiting the use of this resource. Therefore, renewable energy production (i.e. solar energy, geothermal energy) is attracting much attention. Most of those renewable energy resources cannot be economically transformed into electricity by the traditional steam cycle which requires a high-temperature heat source (> 350 °C). Thus, many thermodynamic cycles for converting low-grade heat into electrical power have been studied, i.e. Kalina cycle, Goswami cycle, Trilateral Flash cycle, organic Rankine cycles (subcritical and supercritical Rankine cycle). Among these cycles, Organic Rankine Cycles are less complex and require less maintenance. Therefore these cycles have aroused much interest.

In addition, industrial waste heat recovery is also of great interest. As a matter of fact, industrial sector energy consumption is about 27 % of total world energy consumption (2,282 Mtoe in 2009) (Figure 1.) and many national and international projects are carried out to improve the energy efficiency of the industrial processes.

In practice, a large amount of energy is still lost as waste heat. This waste heat is generated during a combustion process or several other chemical/thermal processes, then is directly evacuated in environment (Tchanche, Lambrinos et al. 2011). In United States of America, 20–50 % or more of energy inputs are possibly lost at the end through flue gases, evaporative or radioactive heat losses and in waste steam and hot water in the

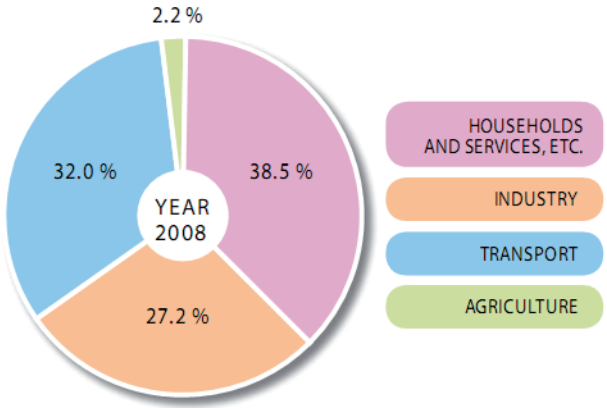

Figure 1. Energy consumption in EU-27 (EU 2011).

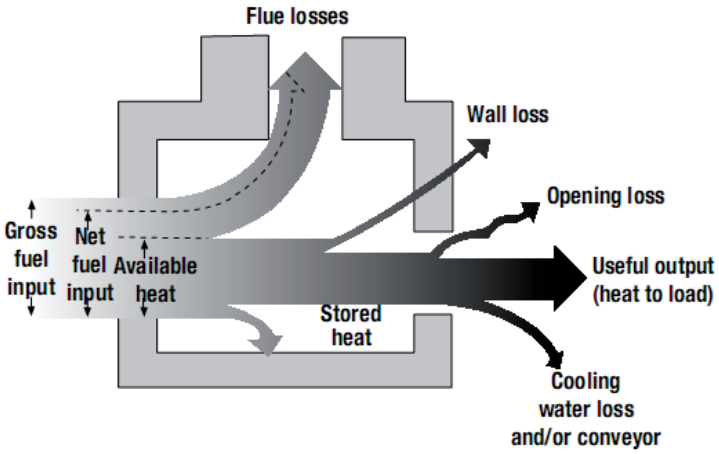

Figure 2. Heat losses in industrial heating processes (source: http://www1.eere.energy.gov).

industrial plants (Pellegrino, Margolis et al. 2004). Many heat losses of an industrial heating process are illustrated in Figure 2. These waste heat sources not only contain an important value of thermal exergy but also a large quantity of pollutants: CO_2, NO_x, SO_x which is responsible for environmental harmful impacts (Global warming, acid rain, etc.). According to the report of U.S Environmental Protection Agency, the energy efficiency of industrial processes can be improved from 10 to 50 % with the heat recovery (EPA 1998).

The heat losses in industrial heating processes in the Figure 2:

- Losses in heat storage in the furnace structure
- Losses from the furnace outside walls or structure
- Heat transported out of the furnace by the load conveyors, fixtures, trays, etc.
- Radiation losses from openings, hot exposed parts, etc.
- Heat losses carried by the cold air infiltration into the furnace
- Heat losses carried by the excess air used in the burners.

The CERES Project

The CERES project is an answer to the need of the energy efficiency and reduction of greenhouse gas emissions in the industry through waste heat recovery. Indeed, the project (2011–2013), supported by the French National Research Agency (ANR), is aimed at developing a decision-making tool to identify the optimal solutions of industrial waste heat recovery. This tool will rely on the simulation of industrial processes and waste heat technologies (modelled in Modelica language) under Open Modelica or Dymola environment and a multi-objectives optimisation platform. The use of the tool will allow the selection of the waste heat recovery solutions according to technico-economic criteria. Several processes from Food and Drink, Metals and Pulp and Paper industries will be studied during the project. Various technical solutions for direct heat recovery (heat exchangers, heat storage, compression and absorption heat pump) or electricity production (thermoelectricity, Organic Rankine Cycles …) will be considered (as illustrated in Figure 3).

Among the technologies studied in the CERES Project, ORC technology is particularly interesting for low temperature waste heat recovery. According to the research of (Lakew and Bolland 2010), many industrial processes and power plants emit waste heat at low-temperature (ca 80–200 °C). This papers describes the work currently done to characterize this technology. In this work, a heat source which is hot air at 170 °C was chosen for simulation of ORC system.

Subcritical organic Rankine cycles

In general, the principle of the Organic Rankine Cycles is the same as that of the steam water Rankine cycle which includes the following components: pump, evaporator, turbine and condenser but the working fluid is often an organic compound (i.e. refrigerants). In this cycle, working fluid at saturated liquid state is pumped to the heat exchanger in which it is heated, vaporized, even superheated by a heat source (i.e. waste heat, thermal oil, hot brine or steam). Then, the vapour at saturated or superheated state is introduced in the turbine linked with an electrical generator to produce the electricity. At the turbine exit, the working fluid is cooled down and condensed by a heat sink (i.e. ambient air or cool water) in the condenser before being introduced in the pump to complete and start again the cycle.

The first organic Rankine cycle was built in 1883, by Frank W. Ofeldt who developed a naphtha engine, i.e. a closed loop steam engine that used naphtha instead of water as working fluid (Towne 1991).

The principle of the subcritical Rankine cycle and T-s diagram of R-245fa are illustrated in Figure 4. In reality, a big superheating of the vapour in subcritical Rankine cycle would not be realized because of the low-exchange coefficient for the gaseous phase (Schuster 2008). Indeed, it is always selected when the critical temperature of working fluid is higher than heat source temperature (Pan, Wang et al. 2012).

Supercritical Organic Rankine cycles

In the state-of-art applications, which are discussed nowadays, saturated or slightly superheated vapour is expanded in the turbine. However, the investigation of the supercritical fluid

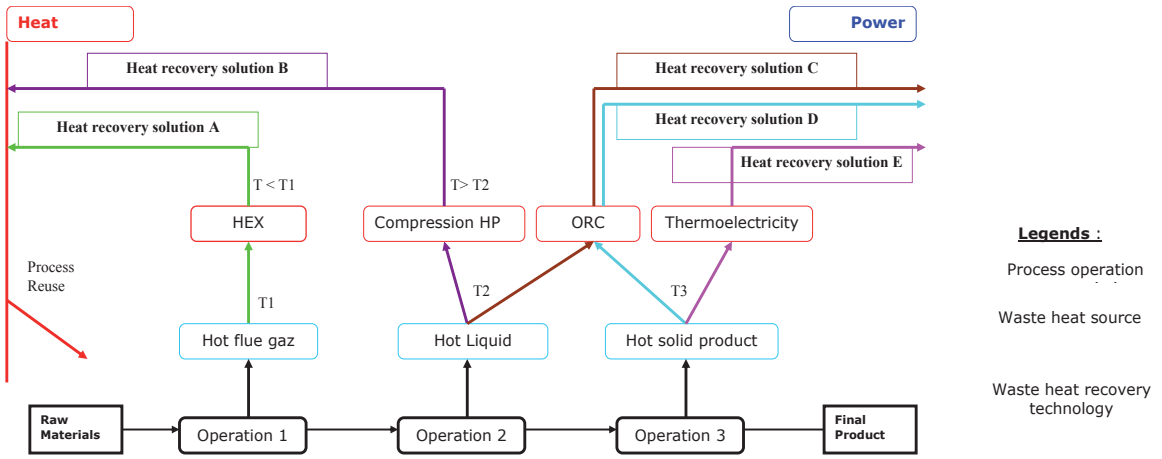

Figure 3. Examples of waste heat recovery solutions according to heat sources.

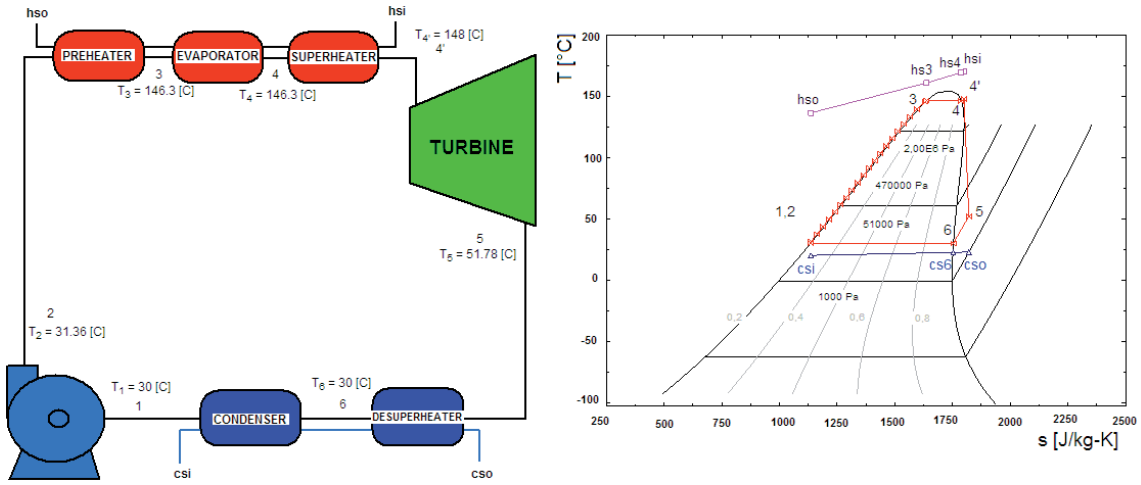

Figure 4. Configuration of a subcritical organic Rankine cycle (left) and T-s diagram of R-245fa (right).

parameters is of high importance, since it may lead to higher efficiencies making these plants even more attractive for waste heat applications (Schuster, Karellas et al. 2010). The working fluid at the exit of the condenser is directly pumped from saturated liquid state to the supercritical pressure in supercritical Rankine cycle (Figure 5). Then, the heating process is realized in the higher temperature heat exchanger by heat absorption of working fluid from heat source. The heating process does not pass through two-phase region like in subcritical Rankine cycle, this result in a better thermal match in the heat exchanger with less irreversibility (Chen, Goswami et al. 2010). When critical temperature of working fluid is far lower than the heat source temperature, supercritical ORC is often selected. In some cases, critical temperature of the fluid is slightly lower than heat source temperature, so both subcritical and supercritical ORC are feasible (Pan, Wang et al. 2012).

The main advantage of the supercritical process is that the average high temperature in which the heat input is taking place is higher than in the subcritical fluid process, leading to a higher efficiency (Schuster 2008). On the other hand, some disadvantages of supercritical Rankine cycle have to be considered, i.e. the difficulties in the operation at high pressure (e.g. 60–160 bars for CO_2 supercritical cycle), the safety concern, and the investment cost rise due to special materials of the system. In present, the supercritical cycle with CO_2 as the working fluid had paid a lot of attention thanks to its desirable properties such as moderated critical point, stability, little environmental impact and low cost. However, the low critical temperature of carbon dioxide is considered like a disadvantage for the condensation process by (Chen, Goswami et al. 2010). Therefore, other working fluids for supercritical Rankine cycle were also studied, i.e. Hydrocarbons (Algieri and Morrone 2012); R134a, R227ea, R152a, R245fa, R236fa (Schuster, Karellas et al. 2010); R32 (Chen, Yogi Goswami et al. 2011) and the mixture fluids (Chen, Goswami et al. 2011).

Working fluids

The selection of the working fluid plays a key role in ORC process and is determined by grade of heat source temperature, ambient temperature or coolant liquid temperature and other criteria (e.g. environmental, economic criteria etc.). Indeed, working fluid properties have a tremendous impact on performance, operating conditions of the ORC system, envi-

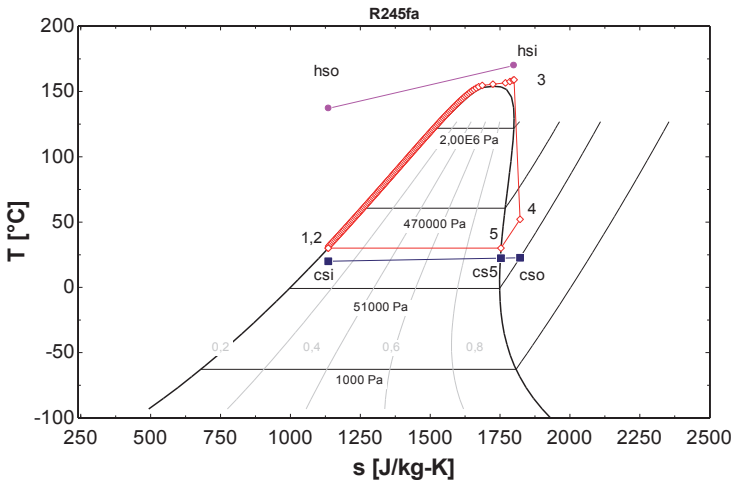

Figure 5. T-s diagram of R-245fa supercritical Rankine cycle.

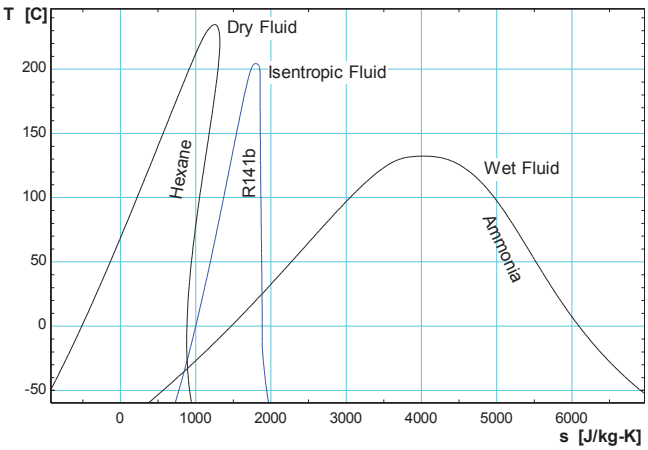

Figure 6. Three types of working fluids: dry fluid, isentropic fluid and wet fluid.

ronmental impact and economic viability (Chen, Goswami et al. 2010). Water is a good working fluid with numerous advantages (i.e. abundant, cheap, high thermal and chemical stability, low viscosity, non-toxicity, non-flammability, zero ODP, zero GWP) but it cannot economically be used for power generation from a low-grade heat source due to its relative high boiling point (99.974 °C, 101.325 kPa). For this purpose, the refrigerants which are essentially organic compounds with low normal boiling temperature present their potentials. Many researchers have focused their study on working fluid selection for ORC system. Predominantly, the system's thermal efficiency and second law efficiency are often used to evaluate working fluid potential.

The organic working fluids are generally categorized into three groups thanks to slope of saturated vapour curve in T-s diagram (Figure 6). The *dry* fluid has a positive slope of saturated vapour curve, the *wet* one – negative, whereas the *isentropic* fluid features a vertical saturation curve. (Liu, Chien et al. 2004) have used ξ (= ds/dT) value (Equation 1) to predict working fluid classification, i.e. $\xi > 0$: dry fluid, $\xi \sim 0$: isentropic fluid and $\xi < 0$: wet fluid.

$$\xi = \frac{C_P}{T_H} - \frac{\frac{n.T_{rH}}{1-T_{rH}} + 1}{T_H^2} \Delta H_H \qquad (1)$$

Where ξ(ds/dT) denotes the inverse of the slope of the saturated vapour curve on T-s diagram; T_{rH} (T_H/Tcrit) denotes the reduced evaporating temperature; ΔH_H represents the enthalpy of fluid vaporization and the exponent n is suggested to be 0.375 or 0.380 (Poling, Prausnitz et al. 2000). The reliability of this equation was verified at the fluid's normal boiling points by Liu, Chien et al. However, the calculations of (Chen, Goswami et al. 2010) based on the definition of the slope (ds/dT) showed that a large deviation can occur when using Equation (1) at off-normal boiling points. These authors recommended using the entropy and temperature data directly to calculate ξ if their values are available.

Due to environmental concerns, CFC working fluids (R-11, R-12, R-113, R-114 and R-115) have been phased out at the end of 1995 (in developed countries) and totally phased-out by 2010 in the developing countries. While HCFC fluids (such as R-21, R-22, R-123, R-124, R-141b and R142b) are being phased out in 2020 (for developed countries) and 2030 (for developing countries) (Government 2011). Many criteria of the refrigerant properties have been proposed for primary screening of working fluids for Organic Rankine Cycles.

Indeed, ideal fluid would have :

- high enough critical point and low enough freezing point,
- acceptable saturation pressure at the temperatures of the application; dry and isentropic fluid are desirable (to avoid excessive superheat in heat exchangers and condensation at the turbine exit) however if slope is too positive, the vapour leaves with substantial superheat which is waste in the condenser; small heat vaporization and matching heat capacity,
- high density, low viscosity,
- high thermal conductivity,
- thermal and chemical stability,
- non-toxic, non-flammable, essentially non fouling, noncorrosive, slight smell, benign to the global physical and biological environment etc.,
- easy leak detection,
- low cost.

The physical data and environmental data of the fluids studied in this work are encapsulated in Table 1.

According to ASHRAE Standard 34 – Designation and Safety Classification of the Refrigerants, the toxicity and flammability classifications of the refrigerants are categorized in six separate safety group classifications (A1, A2, A3, B1, B2 and B3) and two subclasses (A2L and B2L) (Table 2).

A rough procedure which is proposed by (Tettig, Lagler et al. 2011) with the following steps for working fluid selection:

- Literature review on existing organic fluids
- First selection taking into account the working temperature range (heat source and heat sink temperature)

- Second selection with focus on safety and environmental issues (Montreal Protocol)
- Comparison of thermodynamic properties and determination of cycle efficiencies
- Check availability of expansion machines in terms of reasonable operating range

According to critical temperature of working fluids and heat source temperature at 170 °C (443.15 K), some fluids like R141b, R123, R-601, R-600a can only be used for subcritical cycle, while some fluids with lower critical temperature such as R125, R143a, R32, Propane, R22, R1234yf can be preferably used for supercritical applications, whereas the other fluids such as R245fa, R236fa, R142b, R124 present their potential in both applications.

Thermodynamic modelling

The performance of subcritical and supercritical cycle was analyzed and compared via their thermal efficiency and exergy analysis in the present work. Water at ambient temperature (Tcsi = 20 °C) is used to cool down and condense the working fluid. The cycles are calculated for a net power of 1 kW. Turbine isentropic and mechanical efficiency and pump isentropic efficiency are respectively set at 0.87, 0.90 and 0.85. Temperature

Table 1. Physical data and environmental data of refrigerants.

Hydrofluorocarbons (HFCs)	Physical data *				Standard 34 [a] Safety group	Environmental data [a]		
	M [g/mol]	T_b [C]	Tcrit [C]	Pcrit [kPa]		GWP 100 yr	ODP	Atm. life (yr)
HFC-245fa (R245fa)	134.05	15.14	154.01	3651.0	B1	1050	0.000	7.7
HFC-236fa (R236fa)	152.04	-1.44	124.92	3200.0	A1	9820	0.000	242
HFC-152a (R152a)	66.051	-24.023	113.26	4516.8	A2	133	0.000	1.5
HFC-227ea (R227ea)	170.03	-16.34	101.75	2925.0	A1	3580	0.000	38.9
HFC-134a (R134a)	102.03	-26.074	101.06	4059.3	A1	1370	0.000	13.4
HFC-32 (R32)	52.024	-51.651	78.105	5782.0	A2L r	716	0.000	5.2
HFC-143a (R143a)	84.041	-47.241	72.707	3761.0	A2L r	4180	0.000	47.1
HFC-125 (R125)	120.02	-48.09	66.023	3617.7	A1	3420	0.000	28.2
Hydrocarbons (HCs)	Physical data *				Standard 34 Safety group	Environmental data		
	M [g/mol]	T_b [C]	Tcrit [C]	Pcrit [kPa]		GWP 100 yr	ODP	Atm. life (yr)
n-Pentane (R-601)	72.149	36.06	196.55	3370.0	A3	~20	0.000	0.009
n-butane (R-600)	58.122	-0.49	151.98	3796.0	A3	~20	0.000	0.018
Iso-butane (R-600a)	58.122	-11.749	134.66	3629.0	A3	~20	0.000	0.016
Propane (R-290)	44.096	-42.114	96.74	4251.2	A3	~20	0.000	0.041
Hydrochoroflurocarbons (HCFCs)	Physical data *				Standard 34 Safety group	Environmental data		
	M [g/mol]	T_b [C]	Tcrit [C]	Pcrit [kPa]		GWP 100 yr	ODP	Atm. life (yr)
HCFC-141b (R141b)	116.95	32.05	204.35	4212.0	n.a.	717	0.120	9.2
HCFC-123 (R123)	152.93	27.823	183.68	3661.8	B1	77	0.010	1.3
HCFC-142b (R142b)	100.5	-9.12	137.11	4055.0	A2	2220	0.060	17.2
HCFC-124 (R124)	136.48	-11.963	122.28	3624.3	A1	619	0.020	5.9
HCFC-22 (R22)	86.468	-40.81	96.145	4990.0	A1	1790	0.040	11.9
HFO-1234ze (E)	114.04	-18.95	109.37	3636.3	n.a.	6	0.000	0.045
HFO-1234yf (R1234yf)	114.04	-29.45	94.7	3382.2	A2L r	< 4.4	0.000	0.029
Ammonia (R-717)	17.03	-33.327	132.25	11333.0	B2L r	< 1	0.000	< 0.02

*: physical properties of working fluids are calculated by REFPROP 9.0 (Eric 2012)
[a]: (Calm and Hourahan 2011)

Table 2. Six separate group classifications and two subclasses of refrigerants.

	Lower Toxicity	Higher Toxicity	
Higher Flammability	A3	B3	LFL ≤ 0.10 kg/m3 or heat or combustion ≥ 19000 J/kg
Lower Flammability	A2	B2	LFL > 0.10 kg/m3 or heat and combustion < 19000 J/kg
	A2L**	B2L**	
No flame Propagation	A1	B1	No LFL based on modified ASTM E681-85 test
	No identified toxicity at concentrations ≤ 400 ppm	Evidence of toxicitiy below 400 ppm (based on data for TLV-TWA or consistent indices	

**: A2L and B2L are lower flammability refrigerants with a maximum burning velocity of ≤ 10 cm/s

at dead state is 20 °C. Condensation temperature is set at 30 °C. Hot air and cool water flow rate are sequentially 0.2 kg/s and 0.5 kg/s. Each component of these cycles was assumed to be adiabatic. The pressure drop and the heat loss in the pipes and the components of the cycle were neglected. The cycles work in steady flow conditions. The performance calculations and the cycle simulation were carried out by the Engineering Equation Solver (EES) (Klein 2012). The thermodynamic properties of the working fluid were calculated by the built-in functions of EES and the interface FluidProp-EES developed by Thermodynamic Laboratory, University of Liege (Quoilin 2012).

Each component of system is considered to be a control volume. The exergy destruction rate for a steady-flow process is calculated by equation (2).

$$\dot{I} = T_0 \dot{S}_{gen} = T_0 \left(\sum \dot{m}_e s_e - \sum \dot{m}_i s_i - \sum \frac{\dot{Q}_k}{T_k} \right) \quad (2)$$

For the case of an adiabatic process, the equation of exergy destruction rate is rewrote (3):

$$\dot{I} = T_0 \dot{S}_{gen} = T_0 \left(\sum \dot{m}_e s_e - \sum \dot{m}_i s_i \right) \quad (3)$$

The power input and exergy destruction rate of the pump are calculated by following equations for both of sub- and supercritical cycles (Equation 4 and 5).

$$\dot{W}_P = \dot{m}(h_2 - h_1) = \frac{\dot{m}(h_{2,s} - h_1)}{\eta_{s,p}} \quad (4)$$

$$\dot{I}_P = T_0 \dot{m}(s_2 - s_1) \quad (5)$$

In subcritical cycle, the heat absorption process of working fluid from heat source can be imaginarily split into preheating, evaporating and possibly superheating process (to avoid the condensation of working fluid during expansion process) illustrated in Figure 4. While, working fluid, in supercritical cycle, don't pass two-phase region like in subcritical one. It is directly heated from point 2 to point 3 (Figure 5). Total heat received and exergy destruction rate are calculated by following equations:

Subcritical cycle

$$\dot{Q}_{in} = \dot{Q}_{Preheat} + \dot{Q}_{Evap} + \dot{Q}_{superheat} = \dot{m}(h_{4'} - h_2) \quad (6)$$

$$\dot{I}_{HTHEX} = \dot{I}_{Preheat} + \dot{I}_{Evap} + \dot{I}_{superheat} \quad (7)$$

$$= T_0 \left[\dot{m}_h (s_{hso} - s_{hsi}) + \dot{m}(s_{4'} - s_2) \right]$$

In the case without superheating, point 4' will be removed and working fluid enters the turbine at vapour saturated state. Thus, equation (6) and (7) become:

$$\dot{Q}_{in} = \dot{Q}_{Preheat} + \dot{Q}_{Evap} = \dot{m}(h_4 - h_2) \quad (8)$$

$$\dot{I}_{HTHEX} = \dot{I}_{Preheat} + \dot{I}_{Evap} \quad (9)$$

$$= T_0 \left[\dot{m}_h (s_{hso} - s_{hsi}) + \dot{m}(s_4 - s_2) \right]$$

Heat received and exergy destruction rate of higher temperature heat exchanger in supercritical cycle

$$\dot{Q}_{in} = \dot{m}(h_3 - h_2) \quad (10)$$

$$\dot{I}_{HTHEX} = T_0 [\dot{m}_h (s_{hso} - s_{hsi}) + \dot{m}(s_3 - s_2)] \quad (11)$$

Work created by vapour's expansion and exergy destruction rate of turbine is calculated by equations below:

Subcritical cycle

$$\dot{W}_t = \dot{m}(h_{4'} - h_5)\eta_{m,t} = \dot{m}(h_{4'} - h_{5,s})\eta_{s,t}\eta_{m,t} \quad (12)$$

(with superheating)

$$\dot{W}_t = \dot{m}(h_4 - h_5)\eta_{m,t} = \dot{m}(h_4 - h_{5,s})\eta_{s,t}\eta_{m,t}$$

(without superheating)

$$\dot{I}_t = \dot{m}(s_5 - s_{4'}) \quad (13)$$

(with superheating)

$$\dot{I}_t = \dot{m}(s_5 - s_4)$$

(without superheating)

Supercritical cycle

$$\dot{W}_t = \dot{m}(h_3 - h_4)\eta_{m,t} = \dot{m}(h_3 - h_{4,s})\eta_{s,t}\eta_{m,t} \quad (14)$$

$$\dot{I}_t = \dot{m}(s_4 - s_3) \quad (15)$$

Heat exchange and exergy destruction rate in lower temperature heat exchanger:

Subcritical cycle

$$\dot{Q}_{out} = \dot{Q}_{Desuperheat} + \dot{Q}_{Cond} = \dot{m}(h_5 - h_1) \quad (16)$$

$$\dot{I}_{LTHEX} = \dot{I}_{Desuperheat} + \dot{I}_{Cond} \quad (17)$$
$$= T_0\left[\dot{m}(s_1 - s_5) + \dot{m}_c(s_{sco} - s_{sci})\right]$$

Supercritical cycle

$$\dot{Q}_{out} = \dot{Q}_{Desuperheat} + \dot{Q}_{Cond} = \dot{m}(h_4 - h_1) \quad (18)$$

$$\dot{I}_{LTHEX} = \dot{I}_{Desuperheat} + \dot{I}_{Cond} \quad (19)$$
$$= T_0\left[\dot{m}(s_1 - s_4) + \dot{m}_c(s_{sco} - s_{sci})\right]$$

Net power, thermal efficiency and second law efficiency of the cycles are calculated by following equations:

$$\dot{W}_{net} = \dot{W}_t - \dot{W}_P - \dot{W}_{P,water} \quad (20)$$

with

$\dot{W}_{P,water}$ is power input of cool water pump

$$\eta_{th} = \frac{\dot{W}_{net}}{\dot{Q}_{in}} \quad (21)$$

$$\eta_{II} = \frac{\eta_{th}}{\eta_{rev}} = \frac{\eta_{th}}{1 - \frac{\overline{T}_{sc}}{\overline{T}_{hs}}} \quad (22)$$

with

$$\overline{T}_{hs} = \frac{h_{hso} - h_{hsi}}{s_{hso} - s_{hsi}} \text{ and } \overline{T}_{cs} = \frac{h_{cso} - h_{csi}}{s_{cso} - s_{csi}}$$

The heat exchanger effectiveness is calculated by following equation

$$\dot{Q} = \varepsilon \dot{Q}_{max} = \varepsilon \cdot \dot{C}_{min}\left(T_{h,in} - T_{c,in}\right) \quad (23)$$

with

$$\dot{C}_{min} = MIN\left(\dot{m}_h . c_{P,h}; \dot{m}_h . c_{P,h}\right)$$

Performance comparison and exergy analysis

The cycle is operated at evaporating temperature of 90 °C for subcritical configuration and at higher pressure $P_h = 1.03P_{crit}$ for supercritical one. The cycles are flexibly designed to avoid the condensation of working fluid at the turbine exit, a small superheating included if necessary. The results, in Figure 7, show that maximum thermal efficiency (11.99 %) is obtained with Ammonia and minimum one with R227ea (~ 8.95 %) for subcritical cycle; these values become R245fa (14.95 %) and R125 (~ 6.09 %) in the case of supercritical one. But when the total effectiveness of heat exchangers, ε_{tot}, (more effectiveness of heat exchanger, which is calculated according to equation (23), corresponds to more heat exchanger surface area needed) is taken into account, R141b, R142b and R123 are the most appropriate working fluids for subcritical case. Ammonia, a typical wet fluid, needs a big superheating in heat absorption process to avoid vapour condensation which might damage turbine blades during the expansion like in the Figure 8. While, R141b, an isentropic fluid, doesn't need the superheating and its vapour at the turbine exit is nearly saturated vapour. Thus, heat exchange surface area required is much lower than in the case of Ammonia. The alternative fluids such as R245fa, R1234yf also present interests for ORC application. For supercritical case, maximum thermal efficiency is achieved with R245fa and Butane but the total heat exchanger effectiveness is also the most important for these fluids. R125 is not recommended for this case because of its lowest thermal efficiency and a high value of total heat exchanger effectiveness. R142b is always the most appropriate with a relative high thermal efficiency and low total heat exchanger effectiveness.

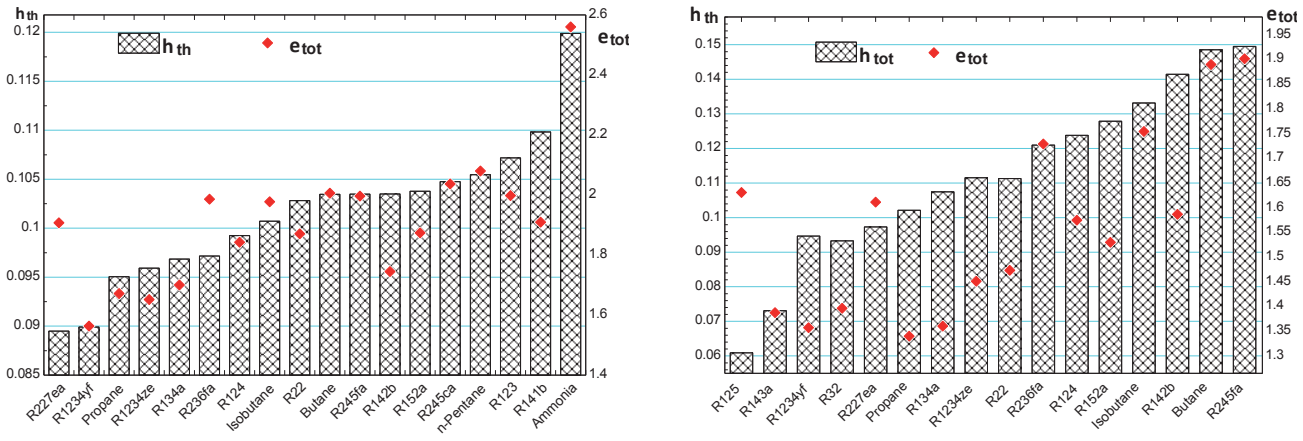

Figure 7. Variation of thermal efficiency (η_{th}) and total heat exchanger effectiveness (ε_{tot}) in function of working fluid in sub- (left) and supercritical Rankine cycle (right).

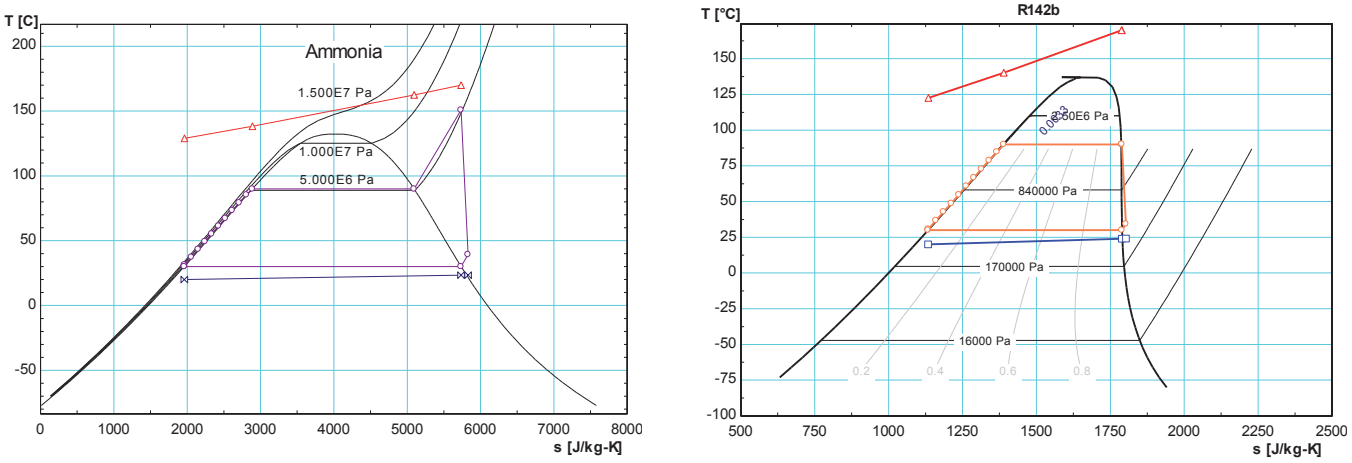

Figure 8. Configuration of subcritical cycle using Ammonia (left) and R141b (right).

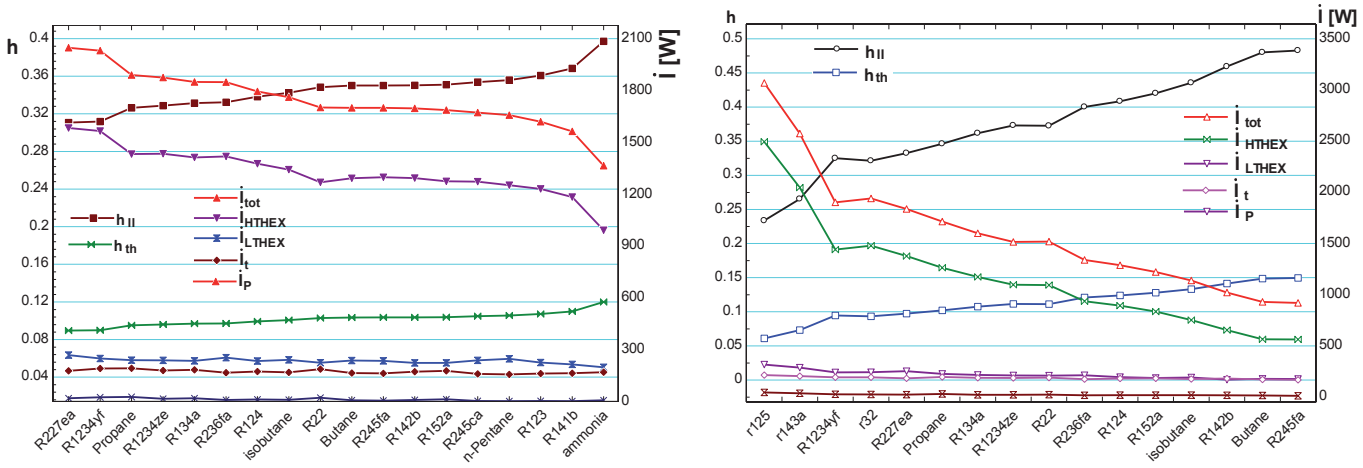

Figure 9. Evolution of exergy destruction rate and second law efficiency in subcritical cycle (left) and supercritical (right) with different working fluids.

In Figure 9, we can observe the evolution of total irreversibility rate and of each component of the cycles. The exergy destruction in higher temperature heat exchanger contributes to the most important part in total exergy destruction. Therefore, curve appearance of $\mathbf{i}_{HTHEX}$ is similar to one of $\mathbf{i}_{tot}$. For the different fluids, exergy destruction rate in lower temperature heat exchanger and in the turbine stays approximately at the same value, while this is relatively different in higher temperature heat exchanger. Pump exergy destruction has the lowest value of all exergy destructions. Second law efficiency grows up with the increase of thermal efficiency and the decrease of total exergy destruction rate.

In Figure 10, we find that evaporating temperature, in subcritical case, and higher pressure, in supercritical case, strongly influence on thermal efficiency. Thermal efficiency is remarkably improved at higher evaporating temperature and higher pressure. This effect is also observed for second law efficiency because heat was being added to working fluid at higher average temperature in these cases. The result is a reduction in the rate of entropy generation and an increase in the efficiency of the cycle.

In Table 3, the results of the comparison between the subcritical cycle and the supercritical one using R245fa are encapsulated. A higher pressure P_h = 1.03Pcrit is applied for supercritical cycle. While, two evaporating temperatures at 140 °C and 150 °C were used in case of subcritical cycle to investigate cycle performance. Inlet turbine temperature and net power are consecutively set at 160 °C and 1 kW for three operating conditions. Back work ratio (bwr), which is defined as the power consumed by the cycle to the gross power produced by the cycle, and the quotient of the higher pressure to the lower one, τ_p, are also studied for two cycles. They are calculated by the equation (24) and (25).

$$bwr = \left(\dot{W}_t + \dot{W}_{P,water} \right) \Big/ \dot{W}_t \qquad (24)$$

$\tau_p = P_h/Pcond$ (for supercritical cycle) (25)
or Pevap/Pcond (for subcritical cycle)

According to these results, supercritical configuration presents numerous advantages such as lower exergy destruction, higher thermal and second law efficiency, less heat exchanger effectiveness required. In other hand, some drawbacks are observed for supercritical cycle, i.e. higher energy consumption, higher

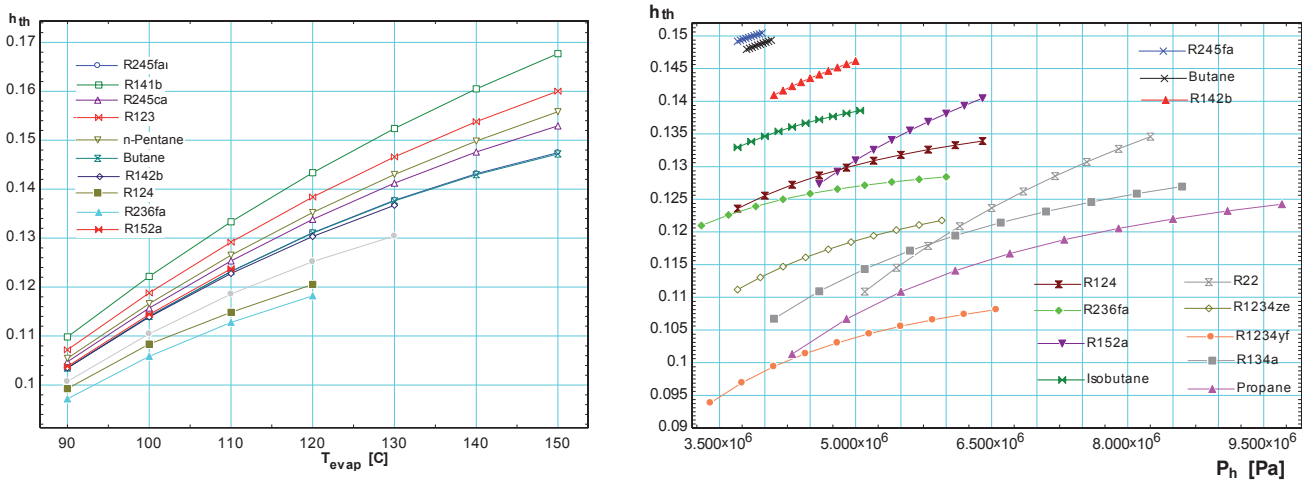

Figure 10. Influence of evaporating temperature (left) in subcritical cycle and higher pressure (right) in supercritical on thermal efficiency.

Table 3. Performance comparison between supercritical and subcritical cycle using R245fa.

	Supercritical cycle	Subcritical cycle	
	P_h = 1.03Pcrit	Tevap = 140 °C	Tevap = 150 °C
ε_{tot}	1.926	2.01	1.977
η_{th}	15.02	14.57	15.01
η_{II}	48.5	47.2	48.47
$\dot{I}_{tot}$ [W]	911.1	970.3	913.8
$\dot{Q}_{in}$ [W]	6657	6861	6662
$\dot{Q}_{out}$ [W]	5510	5717	5516
$\dot{W}_t$ [W]	1106	1081	1094
bwr	0.0962	0.07455	0.08597
τ_P	21.15	15.91	19.09
$\dot{m}$ [kg/s]	0.0260	0.0242	0.0247

operating pressure, so more material resistance required, and more working flow rate needed.

When evaporating temperature in subcritical configuration approaches critical temperature, thermal and second law efficiency in this case close in the efficiencies in case of supercritical cycle. The difference of heat exchanger effectiveness is explained by a bigger superheating in higher temperature heat exchanger and superheated vapour at turbine exit in the case of subcritical cycle compared to the supercritical cycle (Figure 11).

Conclusion

In this work, various working fluids have been studied with subcritical and supercritical configuration of organic Rankine cycle. The results show that, the maximum thermal efficiency is achieved with Ammonia in the case of subcritical configuration but a big undesirable superheating is also required to avoid its vapour condensation during the expansion. R141b, R123 and R142b are the most appropriate fluids with relative high thermal efficiency and low heat exchanger effectiveness in this case. The alternative fluid, i.e. R245fa, present its potential with a relative high thermal efficiency and the desirable properties for the safety and the environment. This fluid gave the

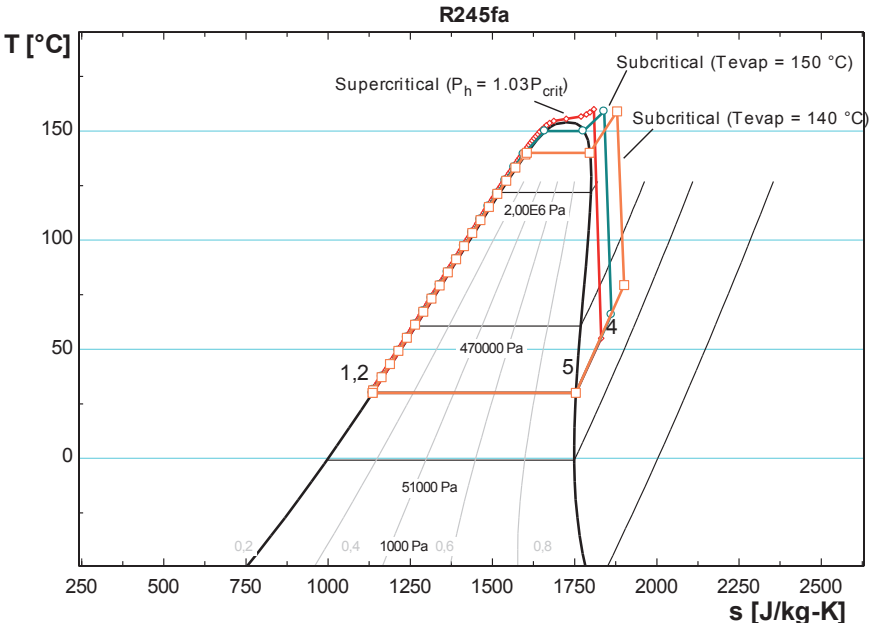

Figure 11. T-s diagram of R245fa with three operating conditions (supercritical cycle with P_h = 1.03Pcrit, subcritical cycle with Tevap = 140 and 150 °C).

maximum thermal efficiency and heat exchanger effectiveness in the case of supercritical configuration. R142b is the most appropriate fluid for supercritical cycle if heat exchanger effectiveness is taken into account. According to exergy analysis, exergy destruction of higher temperature heat exchanger is the most important part of total exergy destruction.

Cycle performance of organic Rankine cycle is improved with supercritical configuration but some disadvantage such as higher operating pressure, higher back work ratio and working flow rate are considered for this case.

The steady-state models with acausal equations, as in the Modelica language, of each ORC components which are developed in EES can be used for thermodynamic simulation by Modelica language later when the fluid properties will be computed using a media library coupled to fluid property databases (e.g. RefProp).

The consequences and coupling of fluid properties on the design and cost of the system remain to be specified. It is the present goal of the continuing study in the labs. The main remark is relative to the availability of the expander, for a specific demand.

Regarding the environment aspect of the fluids data have been given in Table 1, but concerning the cost of fluid, it is today difficult to give precise response to this point; even if we have done demand near of producer, the response seems to be today very sensitive.

Glossary

ACRONYMS

ODP: Ozone depletion potential
GWP: Global Warming potential
LFL: Lower Flammability Limit
ASHRAE: American Society of Heating, Refrigerating and Air-Conditioning Engineers
ASTM: American Society for Testing and Materials

NOMENCLATURE

h: specific enthalpy [kJ.kg^{-1}]

T: Temperature [C]

s: specific entropy [kJ.kg^{-1}.K^{-1}]

P: pressure [Pa]

M: molecular mass (kg/kmol)

bwr: back work ratio

η: efficiency

c_p: specific heat capacity [J.K^{-1}.kg^{-1}]

$\dot{W}$: Power [W]

$\dot{Q}$: Heat rate [W]

$\dot{I}$: Exergy destruction rate (Irreversibility rate) [W]

$\dot{C}$: Heat capacity rate

$\dot{m}$, $\dot{m}_h$, $\dot{m}_c$: Flow rate of working fluid, hot air and cool water [kg/s]

SUB- AND SUPERSCRIPT

hs: Heat source inlet
cs: Cold source (heat sink)
th: Thermal
rev: reversible
II: second law
Evap: Evaporation
Cond: Condensation
LTHEX: Lower temperature heat exchanger
HTHEX: Higher temperature heat exchanger

in, i: Inlet
out, o: Outlet
sub: Subcritical
super: Supercritical
0: Dead state (reference state)
t: Turbine
p: Pump
P: Pressure
h: higher or hot fluid
b: boiling point
crit: critical
tot: total
c: cold fluid

References

Algieri, A. and P. Morrone (2012). "Comparative energetic analysis of high-temperature subcritical and transcritical Organic Rankine Cycle (ORC). A biomass application in the Sibari district." *Applied Thermal Engineering* **36**: 236-244.

Calm, J. M. and G. C. Hourahan (2011). Physical, Safety, and Environmental Data for Current and Alternative Regrigerants. *The 23rd International Congress of Refrigeration* Prague, Czech Republic, International Institute of Refrigeration (IIR/IIF).

Chen, H., D. Y. Goswami, et al. (2011). "A supercritical Rankine cycle using zeotropic mixture working fluids for the conversion of low-grade heat into power." *Energy* **36**(1): 549-555.

Chen, H., D. Y. Goswami, et al. (2010). "A review of thermodynamic cycles and working fluids for the conversion of low-grade heat." *Renewable and Sustainable Energy Reviews* **14**(9): 3059–3067.

Chen, H., D. Y. Goswami, et al. (2011). "Energetic and exergetic analysis of CO2- and R32-based transcritical Rankine cycles for low-grade heat conversion." *Applied Energy* **88**(8): 2802–2808.

EPA (1998). Climate wise. Wise Rules for Industrial Efficiency: A Tool Kit for Estimation Energy Savings and Greenhouse Gas Emissions Reductions**:** 18.

Eric, W. L. (2012). "NIST Standard Reference Database 23." from http://www.nist.gov/srd/nist23.cfm.

EU (2011). *EU transport in figures*, European Union.

Government, A. (2011, 07/04). "Australia and the Montreal Protocol on Substances that Deplete the Ozone Layer." from http://www.environment.gov.au/atmosphere/ozone/legislation/montp.html.

IEA (2011). Key World Energy Statistics**:** 37.

IEA (2011). *World Energy Outlook 2011*, International Energy Agency.

Klein, S. A. (2012). "EES: Engineering Equation Solver | F-Chart Software : Engineering Software." from http://www.fchart.com/ees/.

Lakew, A. A. and O. Bolland (2010). "Working fluids for low-temperature heat source." *Applied Thermal Engineering* **30**(10): 1262–1268.

Liu, B.-T., K.-H. Chien, et al. (2004). "Effect of working fluids on organic Rankine cycle for waste heat recovery." *Energy* **29**(8): 1207–1217.

Pan, L., H. Wang, et al. (2012). "Performance analysis in near-critical conditions of organic Rankine cycle." *Energy* **37**(1): 281–286.

Pellegrino, J. L., N. Margolis, et al. (2004). Energy Use, Loss and Opportunities Analysis: U.S. Manufacturing & Mining**:** 17.

Poling, B. E., J. M. Prausnitz, et al. (2000). *The Properties of Gases and Liquids*, McGraw-Hill Professional.

Quoilin, S. (2012). "Labothap – EES Fluidprop Interface." from http://www.labothap.ulg.ac.be/cmsms/index.php?page=ees-fluidprop-interface.

Schuster, A., S. Karellas, et al. (2010). "Efficiency optimization potential in supercritical Organic Rankine Cycles." *Energy* **35**(2): 1033–1039.

Schuster, S. K. a. A. (2008). "Supercritical fluid parameters in organic rankine cycle applications." *International Journal of Thermodynamics* **11**(3): 101–108.

Tchanche, B. F., G. Lambrinos, et al. (2011). "Low-grade heat conversion into power using organic Rankine cycles – A review of various applications." *Renewable and Sustainable Energy Reviews* **15**(8): 3963–3979.

Tettig, A., M. Lagler, et al. (2011). Application of Organic Rankine Cycles (ORC). *World Engineers' Convention*. Geneva, Sweden.

Towne, P. (1991). "The Naphtha Engine." 2012, from http://gasengine.farmcollector.com/Gas-Engines/The-Naphtha-Engine.aspx.

Acknowledgements

The work reported in this paper is funded by the French National Research Agency.